AGU PUBLICATIONS

Geophysical Research Letters

RESEARCH LETTER
10.1002/2015GL063083

Key Points:
- SST anomalies in the Pacific were a primary cause of the severe winter of 2014
- Warmth in the tropical west Pacific led to cold in central North America
- Specified SST model experiments replicate the observed teleconnections

Supporting Information:
- Readme and Figures S1–S5

Correspondence to:
D. L. Hartmann,
dhartm@washington.edu

Citation:
Hartmann, D. L. (2015), Pacific sea surface temperature and the winter of 2014, *Geophys. Res. Lett.*, *42*, 1894–1902, doi:10.1002/2015GL063083.

Received 8 JAN 2015
Accepted 17 FEB 2015
Accepted article online 19 FEB 2015
Published online 19 MAR 2015

Pacific sea surface temperature and the winter of 2014

Dennis L. Hartmann[1]

[1]Department of Atmospheric Sciences, University of Washington, Seattle, Washington, USA

Abstract It is shown from historical data and from modeling experiments that a proximate cause of the cold winter in North America in 2013–2014 was the pattern of sea surface temperature (SST) in the Pacific Ocean. Each of the three dominant modes of SST variability in the Pacific is connected to the tropics and has a strong expression in extratropical SST and weather patterns. Beginning in the middle of 2013, the third mode of SST variability was two standard deviations positive and has remained so through January 2015. This pattern is associated with high pressure in the northeast Pacific and low pressure and low surface temperatures over central North America. A large ensemble of model experiments with observed SSTs confirms that SST anomalies contributed to the anomalous winter of 2014.

1. Introduction

Much interest has focused on the very cold winter in the central and eastern U.S. and Canada in 2013–2014 (hereafter the winter of 2014). It has been suggested that melting of polar sea ice could be responsible for causing unusual weather events (*Francis and Vavrus* [2012] but see *Barnes* [2013]), perhaps through the intermediacy of stratospheric warmings [*Kim et al*., 2014]. This would be remarkable given the small area of the Arctic Ocean and its presence at the tail end of the atmospheric and oceanic chain moving energy from the tropics toward the poles. Taking a different perspective, *Ding et al*. [2014] use models and observations to show that at least some of the recent Arctic warming has been forced by changes in the tropical Pacific. Here the coupled variability between the Pacific Ocean and the global atmosphere is used to account in part for the unusual winter of 2014. Using a combination of analysis of past data and a large ensemble of specified sea surface temperature (SST) modeling experiments, a strong case can be made that variability of the ocean-atmosphere system originating in the tropics is the most likely "cause" of the winter of 2014 anomalies.

The ocean provides the long-term memory for the climate system through its higher heat capacity, slowly varying large-scale modes, and long adjustment time to changes in forcing. The El Niño–Southern Oscillation (ENSO) phenomenon is a coupled ocean-atmosphere phenomenon that is the dominant mode of interannual variability globally and has provided the opportunity to make useful forecasts of seasonal weather and climate conditions a season or more in advance [*Neelin et al*., 1998; *Rasmusson and Wallace*, 1983]. ENSO has a related decadal variability, the Pacific Decadal Oscillation (PDO), which was first defined in terms of North Pacific sea surface temperature (SST) anomalies [*Mantua and Hare*, 2002; *Zhang et al*., 1997], and is now thought to influence global mean temperature on decadal time scales [*Huber and Knutti*, 2014; *Kosaka and Xie*, 2013; *Trenberth and Fasullo*, 2013]. Interannual anomalies of SST are known to have a significant influence on climate over land, and these relationships play an important role in seasonal climate forecasting [*Palmer and Anderson*, 1994] and in the explanation of drought [*Seager and Hoerling*, 2014]. While the connection between tropical SST anomalies and winter weather in the extratropics is well established [*Horel and Wallace*, 1981], SST anomalies in middle latitudes are driven by atmospheric anomalies and it is more difficult to show an influence of extratropical SST anomalies in driving atmospheric anomalies [*Kushnir et al*., 2002; *Lau and Nath*, 1994]. The extratropical SST anomalies associated with ENSO are caused primarily by atmospheric anomalies propagating from the tropics [*Alexander et al*., 2002].

In this paper we explore anomalies in monthly mean SST in the Pacific and their relation to recent weather anomalies. We first present a decomposition of Pacific Ocean SST variability into three key modes: ENSO, which has its strongest variability on time scales of 2 to 6 years, and two decadal modes that are related to ENSO and have a strong expression in the North Pacific. We next relate these SST patterns to atmospheric variability and show that one of the decadal modes is associated with atmospheric anomalies that look very

much like those during the winter of 2014. This mode of variability showed a positive anomaly of two standard deviations beginning in the summer of 2013. To demonstrate a causality relationship between this large anomaly in the SST mode and the winter of 2014, we analyze a large ensemble of specified SST modeling experiments. Since these specified SST experiments produce anomalies with similar structure and amplitude to the observed anomalies in 2014, we conclude that SST variations rooted in the tropics played a key role in producing the cold winter of 2014.

2. SST Variability: ENSO, PDO, and North Pacific Mode

The Pacific Decadal Oscillation (PDO) has classically been defined as the first empirical orthogonal function (EOF) of the anomalies of monthly mean SST poleward of 20°N in the Pacific Ocean [*Mantua et al*., 1997]. *Bond et al*. [2003] noted that the second EOF of North Pacific SST was anomalously negative in 1999–2002 and emphasized that the PDO alone is not sufficient to characterize the variability of the North Pacific. Here we include the ocean region from 30°S to 65°N and 120°E to 105°W, which includes the tropical and North Pacific. We use the NOAA Extended Reconstructed Sea Surface Temperature (ERSST) data set [*Smith et al*., 2008] to compute the EOF decomposition after removing the seasonal cycle, the global mean, and the linear trend from the monthly data. We have obtained similar results with the Hadley Center Sea Ice and SST Data Set (HadISST) [*Rayner et al*., 2003] (not shown). Although the data set starts in 1854, we focus on the period since 1900 when the data are more complete. The first EOF expresses about 30% of the variance, and the next two modes each express about 8% of the variance (Figure S1 in the supporting information). The second and third modes are not distinguished from each other by their explained variance [*North et al*., 1982], and their relative rankings will change for different sampling periods. For example, the third mode for the period from 1900 becomes the second mode in the period since 1979. The remaining EOFs form a continuum of modes that are not distinguished from each other by their explained variance. The SST modes shown here are for all 12 months, but the basic structures are the same if winter or summer half years are used instead. The structures and explained variances are very similar if we use instead only the period since 1950, when the observational network had improved further. The first three SST modes are shown in Figure 1 as regressions of the SST anomalies with the principal component time series of each mode. The first mode captures much of the equatorial variance, but the second and third modes also have significant connections to the tropics.

In the supporting information we show that these three modes are related to each other (Figure S2). The second mode tends to become strongly positive after a warm ENSO event. This expresses the fact that the extratropical signature of a warm event, which gives cold SST in midlatitudes via the "atmospheric bridge" [*Lau and Nath*, 1996], tends to persist longer than ENSO itself. So its structure is cold in midlatitude western Pacific and also cold in the eastern equatorial Pacific. The third mode tends to be in its positive phase prior to ENSO warm events and is closely related to the "footprinting" mechanism [*Vimont et al*., 2001, 2003]. The structures of the second and third modes in Figure 1 appear to be dominated by amplitude away from the equator, but they are nonetheless connected to the tropics. The variance of SST is large in the North Pacific (not shown), so the regressions are large there, but both the correlation patterns associated with these two modes and their strong temporal relationship to ENSO indicate their tropical roots.

During the satellite era since 1979, the third mode has been very strong, and it enters as the second mode of global SST during that period (not shown). In the classical analysis of the PDO using the region poleward of 20°N [*Mantua and Hare*, 2002], the first mode is that identified as the PDO, while the second mode is very similar to the third mode for the larger domains employed here. *Deser and Blackmon* [1995] referred to the second mode SST structure as the North Pacific Mode (NPM). The NPM mode is very robust to the region used. It appears as the second mode for the Pacific region north of 20°N, one of two modes centered in the North Pacific for the Pacific Ocean north of 30°S shown here, and also as the second mode of global SST for the period since 1979.

The extratropical signatures of the second and third modes in Figure 1 may be influenced by the North Pacific Gyre Oscillation [*Ceballos et al*., 2009; *Chhak et al*., 2009; *Di Lorenzo et al*., 2008] and by fluctuations in the Kuroshio and Oyashio Currents [*Frankignoul et al*., 2011; *Kwon et al*., 2010]. *Seager et al*. [2001] performed an ocean heat budget analysis in the Kuroshio-Oyashio Extension region and showed how surface fluxes, Ekman current-induced ocean heat convergence, and Rossby wave adjustment combine to generate the SST anomalies. Thus, both atmospheric forcing and the oceanic dynamic response are important for the

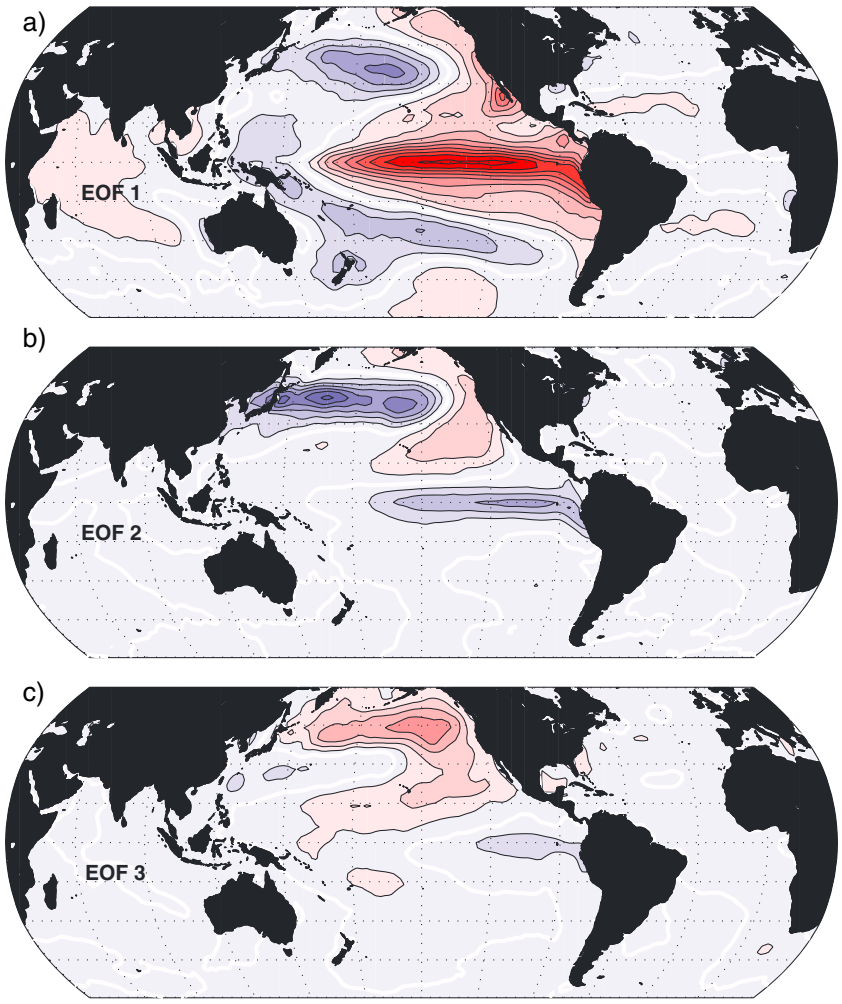

Figure 1. The regressions of monthly mean anomalies of global SST onto the first three EOFs of SST for the ocean area 30°S–65°N, 120°E–105°W and the period from January 1900 to July 2014. Contour interval is 0.1°C. Positive values are red, negative values are blue, and the zero contour is white. Robinson projection from 60°S to 60°N.

evolution of the North Pacific SST and surface height [e.g., *Miller et al*., 1998; *Vivier et al*., 1999; *Qiu*, 2000; *Cummins and Freeland*, 2007]. Local atmospheric forcing seems to be very important in the North Pacific at least on seasonal and interannual time scales, and both local and remote influences may be important [*Alexander et al*., 2002; *Liu and Alexander*, 2007]. *Smirnov et al*. [2014] conclude that internal ocean dynamics play little role in interannual SST variability in the eastern Pacific in comparison to the western Pacific where the Kuroshio and Oyashio Currents may play a more important role.

The principal components of the first three EOFs are shown in Figure 2 in units of standard deviations for the period from 1979 to January 2015. These EOFs are based on the Pacific north of 30°S during the period from 1900 to 2014. During the most recent period shown in Figure 2, hints of the relationships between the three EOFs during warming events can be seen. Both the second and third modes show large-amplitude variations associated with major warming events. Since the 1998 warm ENSO event, the principal components of the first two EOFs have been mostly negative, which is a reflection of the tendency for cool ENSO and negative PDO since then. After May 2013, however, the first two EOFs were near neutral amplitude, while the third EOF (NPM) maintained a positive value near two standard deviations above neutral. Unusually warm temperatures in the northeast Pacific prevailed during this period.

The very high SST anomaly in the North Pacific that emerged in May 2013 is linked to reduced cooling of the ocean during the prior winter of 2013. The SST, heat content, surface wind stress, and surface heat flux

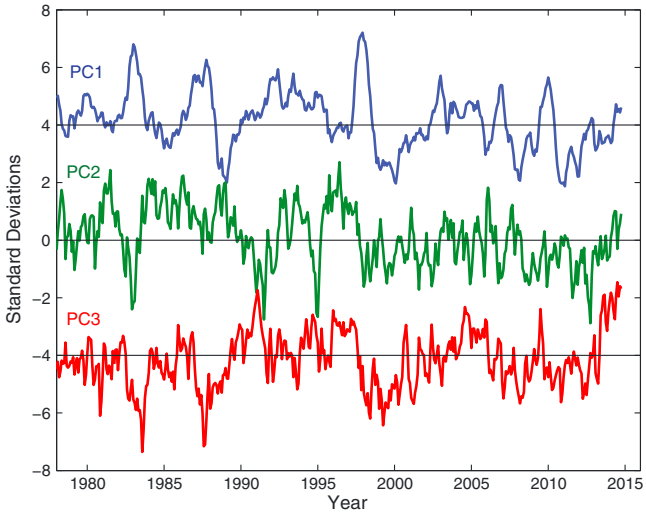

Figure 2. Time series of the principal components of the first three EOFs of monthly mean Pacific SST poleward of 30°S as shown in Figure 1. Only values from January 1979 to January 2015 are shown. Units are standard deviations. Values are offset by four standard deviations for clearer viewing.

anomalies for 2013 are well illustrated in the State of the Climate 2013 report [*Blunden and Arndt*, 2014], particularly in Figures 3.1 to 3.9 of *Newlin and Gregg* [2014]. These show strongly suppressed wind stresses and positive anomalies of surface heat fluxes into the North Pacific Ocean during 2013. It is likely that these anomalies are rooted in the tropics, but it is important to confirm what caused these anomalous fluxes in 2013 and to what extent the heat stored then influenced the weather of the following winter.

3. Meteorological Connections to Pacific SST Anomalies

We have regressed the monthly principal components of the first three EOFs of SST on the 500 hPa height and lowest model level temperature from both the Twentieth Century Reanalysis that starts in 1871 [*Compo et al*., 2011] and the National Centers for Environmental Prediction (NCEP)/National Center for Atmospheric Research (NCAR) Reanalysis that starts in 1948 [*Kalnay et al*., 1996]. We obtain similar results from both reanalysis data sets and from shorter subsets of each data set. For the sake of brevity we show the results for the NCEP/NCAR Reanalysis.

Since the focus of this paper is the influence of the North Pacific Mode on the winter of 2014, we will show only the regression for that mode here, but correlation patterns for all three modes are shown in the supporting information (Figure S3). Figure 3a shows the anomaly of the 500 hPa field for November 2013 to March 2014, the winter of 2014. It shows a ridge over the North Pacific and a deep trough over the central North America centered just south of Hudson Bay. The northerly flow between these two centers, which is roughly aligned with the Rocky Mountains, brought cold Arctic air into central North America and gave unusually cold conditions there.

Figure 3b shows the regression of the global 500 hPa height field from NCEP/NCAR reanalysis during months of November through March onto the second principal component of global SST based on the period from 1979. The second mode of global SST for 1979 to 2014 is very similar to the third mode of SST for the period 1900 to 2014 shown in Figure 1. Figure 3b is not very different when based on the SST since 1900 and the NCEP/NCAR data since 1948, but we show the satellite era data to be consistent with the model simulations discussed later. The regressions show the amplitude explained by a one-standard deviation variation of the principal component. A large high pressure occurs over the northern Pacific centered near the Aleutian Islands with a downstream low centered near Hudson Bay. These are connected to a low along 30°N over the Pacific Ocean.

Figure 4 shows the same anomalies and regressions as in Figure 3, except for the temperature anomalies at the lowest model level. During the winter of 2014 extreme cold anomalies persisted across North America while warm anomalies persisted in the northeast Pacific and in Alaska. These anomalies are also reflected in the regression of the North Pacific Mode of SST onto the low-level temperatures in Figure 4b. The regression shows a maximum cold anomaly of about 1°C over North America for one standard deviation departure of the NPM; so for two standard deviations of the NPM SST, the regression predicts a surface temperature anomaly of about 2°C over North America, which is close to the 2.6°C anomaly in Figure 4a.

The statistical significance of the features in the regression plots shown here is assessed by determining whether the correlations associated with them are different from zero at the 95% level. The degrees of freedom have been determined using the approximation recommended by *Bretherton et al*. [1999]. Although

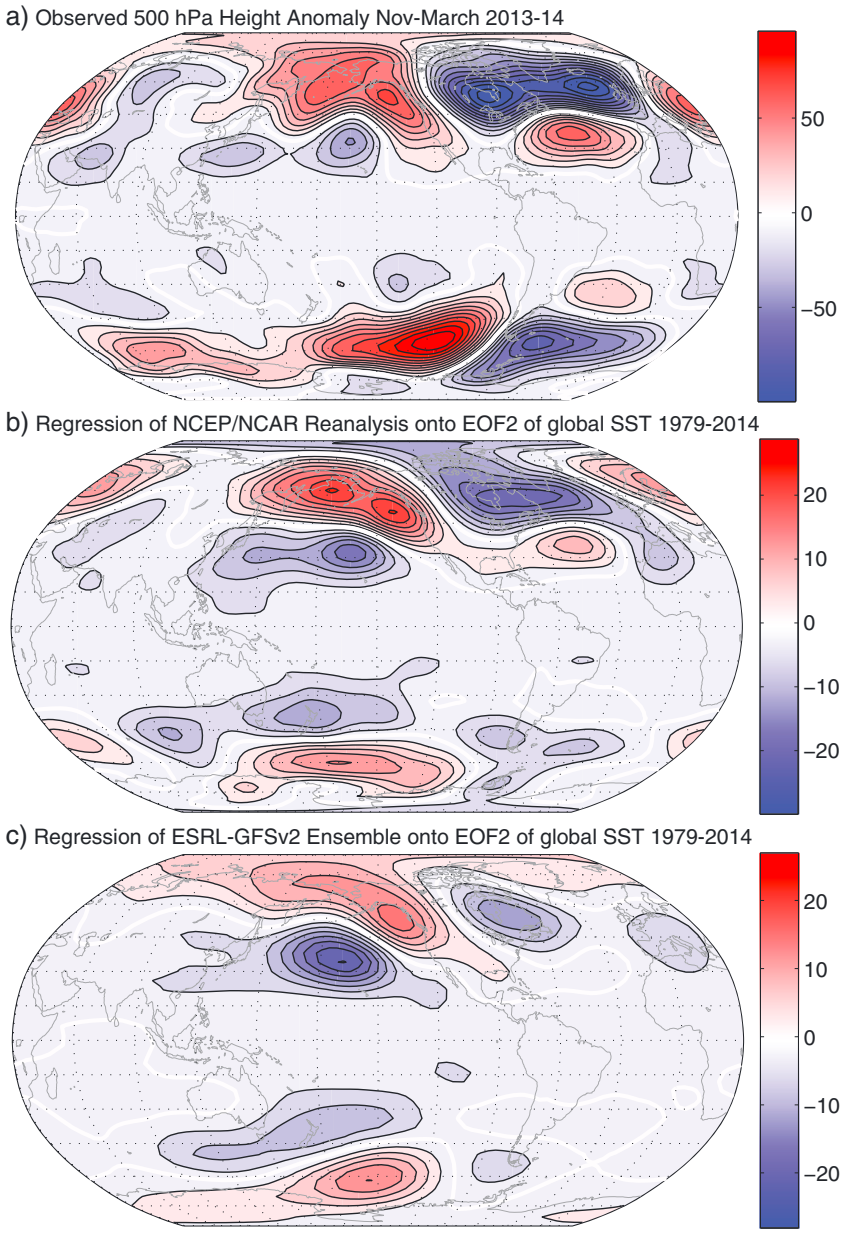

Figure 3. (a) The observed anomaly in 500 hPa height for November 2013 to March 2014 (contour interval is 10 m, positive is red, negative is blue, and the zero contour is white). (b) Regression of the 500 hPa height anomalies for the months of November to March for the years from 1979 to 2014 onto the principal component time series for the second EOF of global SST for the period from 1979 to 2014 (contour interval is 3 m). (c) Same as Figure 3b, except that the height data are from the 50-member ensemble from the Earth System Research Laboratory-Global Forecast System version 2 (ESRL-GFSv2) using the observed SST.

the SST indices are highly autocorrelated, the extratropical height anomalies are not, so that for the 67 year record from 1948 and the 5 months of November to March, the data used to perform the height regressions possess about 250 degrees of freedom. For the record since 1979, the degrees of freedom still number 130. With this large number of degrees of freedom, relatively small correlations become significant, and the question shifts to whether the fraction of variance explained is interesting or not. Thus, the absolute values of the correlation coefficients are of more interest than their proven statistical significance. The correlation coefficient map corresponding to Figures 3b and 4b have correlations between 0.3 and 0.4 for the centers over North America. For comparison, the correlations associated with the ENSO mode exceed 0.6 in the

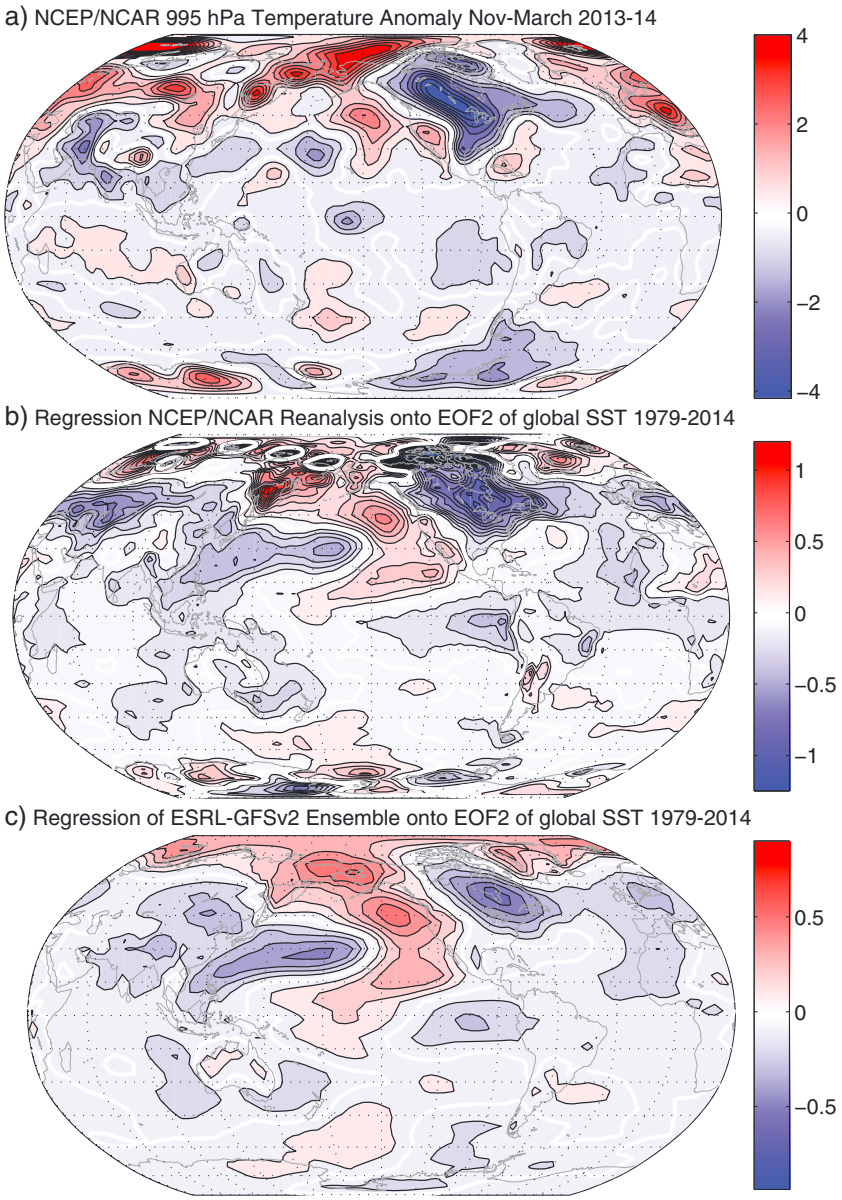

Figure 4. The same as Figure 3, except that the variable plotted is the temperature at the lowest model level. Contour interval is (a) 0.5 and (b and c) 0.1.

extratropics for SST EOFs computed from both the global and Pacific regions. We therefore conclude that the winter of 2014 over North America was favored by the prevailing NPM SST anomaly pattern over the Pacific Ocean.

Wang et al. [2013] explore the influence of SST modes on North American weather. They estimate that the three leading modes they consider explain about 50% of the total effect of SST on North American climate, but the modes they considered in the Pacific correspond roughly to the ENSO mode and the PDO mode (or Kuroshio extension mode), and they do not consider the NPM described here. Since our analysis shows that the second and third modes explain the same amount of variance, any linear combination of the two is as valid a representation as either mode alone. Since the third mode reaches large amplitude during the period of interest, while the first and second modes are near neutral, it is meaningful to consider only the third mode in detail here.

The pattern of SST and height variability we find with the NPM is similar to the structure that *Seager et al*. [2014] associate with the California drought, particularly during the November 2013 to April 2014 period. They used model experiments with specified SST to show that these anomalies are keyed to warm SST anomalies in the tropical Pacific west of the dateline. The ridge-trough pattern over North America suppresses precipitation in California while it also induces cold anomalies in the middle of the continent. We emphasize the cooling effect here. It should be noted that the prior two winters of 2011–2012 and 2012–2013 were not strong positive NPM years (Figure 1). The ridge was farther west offshore, and the deep trough over North America was much less developed. The drought during those years was more likely associated with the strong La Niña conditions during the 2011–2012 winter, with continued warm SST in the western equatorial Pacific the following year, and the strongly positive NPM mode in 2013–2014 completed 3 years of intense drought in California.

Similarly, *Wang et al*. [2014] associated the California drought of 2013–2014 with the anomaly height pattern for November-December-January, which is very similar in structure to Figure 3. They focused particularly on the dipole pattern between the ridge in the Gulf of Alaska and the trough centered just south of Hudson Bay. They found that this pattern was correlated with the Niño4 SST index, 1 year prior. In general outline this is consistent with our conclusion that the winter of 2014 pattern is associated with a precursor mode of ENSO. *Wang et al*. [2014] go on to conclude that this pattern is becoming more prevalent in consequence of human-induced warming of the climate. *Seager et al*. [2014] conclude that the California drought is largely a natural variability and has precedents in earlier times. We do not investigate any connections to climate change in this paper.

4. Specified SST Experiments

So far, it has been demonstrated that the structure that dominated the winter weather in North America in 2014 is similar in shape and slightly smaller than the regression onto the NPM SST pattern that dominated in that year. To make a stronger case that the SST anomaly caused some important part of the weather anomaly, rather than merely being associated with it, we turn to Atmospheric Model Intercomparison Project (AMIP)-style experiment data provided by the NOAA-ESRL Physical Sciences Division, Boulder, Colorado, from their website at http://www.esrl.noaa.gov/psd/repository/alias/facts/. The experiments chosen apply the observed radiative forcing and specify the observed SSTs under an atmospheric model. Large ensembles of experiments starting in 1979 were conducted with several different models of the atmosphere. Three model ensembles are considered here; a 50-member ensemble with the ESRL-GFSv2 model, a 30-member ensemble with the fifth-generation European Centre/Hamburg (ECHAM5) model, and a 20-member ensemble with the Community Atmosphere Model 4 (CAM4). We use the ensemble mean anomalies for each model to both regress them onto the SST indices. To be consistent with our data analysis, we remove the linear trend.

Figure 3c shows the regression of the 500 hPa height anomalies for the ESRL-GFSv2 50-member ensemble mean onto the NPM mode. The ECHAM5 and CAM4 models produce similar results (Figure S5). The predicted anomaly has key features in common with the observed anomaly in Figure 3a but with smaller amplitudes. The depth of the low at about 35°N in the central Pacific is well simulated, but the ridge on the West Coast and especially the downstream low over North America are much attenuated compared to the observed regression pattern in Figure 3b.

Figure 4c shows the corresponding regression for the simulation of the temperature at the lowest model level. The story is very similar to that for the 500 hPa height. The regression of the simulated temperatures onto the NPM SST mode captures many of the key features of the anomalies of 2013–2014, especially the cold conditions over North America. The regression pattern produced by the AMIP simulations has a much weaker cool anomaly over North America than for the regression on observations. It is unclear why the models underestimate the observed connections between SST and North American weather. The model resolution in these experiments is 0.75 to 1°, and it is possible that the wave pattern is sensitive to the resolution of the Rocky Mountains, which are smoothed somewhat in these simulations.

In future work we could look to see if a significant number of the ensemble members do get the observed downstream amplitude in 2014, but that is an additional data processing chore. It is important to remember that fixed SST experiments do not capture the full interaction between the atmosphere and ocean [*Barsugli and Battisti*, 1998], and simple interpretations of ensembles often underestimate the confidence of seasonal

predictions [*Eade et al.*, 2014]. For the 1979 to 2014 period there is little difference between the regression on the global SST pattern and the NPM pattern for the Pacific north of 30°S. Although the winter of 2014 was a 2 sigma event in terms of the NPM of SST, the regressions with NCEP/NCAR Reanalysis include 35 (or 67 for the period since 1948) winters and are not very sensitive to the inclusion or not of the winter of 2014.

5. Discussion and Conclusion

It appears that the sudden increase in the NPM SST anomaly pattern in the North Pacific during the middle of 2013 can be associated with the subsequent cold winter in the center of North America. Although the pattern of SST anomaly is very strong in the North Pacific, it is virtually certain that the forcing for these anomalies originates with warm SST in the tropical west Pacific. Preliminary experiments indicate that the atmospheric pattern during the winter of 2014 is not efficiently forced by the extratropical SST anomalies but can be generated with the observed warm SST anomalies in the tropical west Pacific (P. Ceppi, personal communication, 2015). This result is consistent with a long history of observational and modeling work indicating that SST anomalies in the extratropics are strongly driven by atmospheric circulation anomalies [*Cayan*, 1992; *Davis*, 1976], while SST anomalies in the tropics can strongly force the atmospheric circulation [*Lau and Nath*, 1994].

The NPM mode of SST variability remains strongly positive as of this writing in January 2015, and its future evolution will be interesting to watch. The reasons why the NPM anomalies arose so strongly in the middle of 2013 remain to be explored. The stage was set for the very positive NPM extratropical SST anomaly of the 2014 winter by a reduction in heat extraction from the North Pacific in the prior winter of 2013. The annual mean 500 hPa anomaly for 2013 shows a large high pressure over the North Pacific centered at about 50°N, 150°W (not shown). Generally, warm anomalies of the SST in the tropical western Pacific have persisted since the winter of 2013 (http://www.esrl.noaa.gov/psd/map/clim/sst.shtml).

Midlatitude seasonal weather and climate anomalies receive a large contribution from internal atmospheric variability that is unrelated to any interactions with the SST [e.g., *Deser et al.*, 2012]. The effect of ocean heat anomalies and associated SST anomalies on the seasonal weather patterns can thus be negated by other variability in any particular month. Nonetheless, the systematic connection between NPM SST anomalies and winter weather in the past, the extreme amplitude of the SST anomalies in 2013–2014, and the similarity of the 2014 winter anomalies to the historical pattern all suggest that the warm SST in the tropical and North Pacific likely made a significant contribution to the cold winter in central North America in 2013–2014. Specified SST simulations with three models confirm the causal relationship between the NPM SST mode and winter weather in North America.

Acknowledgments

The SST data were obtained from the NOAA ERSST data set at http://www.esrl.noaa.gov/psd/data/gridded/data.noaa.ersst.html. Twentieth Century Reanalysis and NCEP/NCAR Reanalysis products were obtained from the NOAA websites http://www.esrl.noaa.gov/psd/data/20thC_Rean/ and http://www.esrl.noaa.gov/psd/data/gridded/data.ncep.reanalysis.html. AMIP simulations from the NOAA website http://www.esrl.noaa.gov/psd/repository/alias/facts/ were crucial to this analysis. This work was supported by NSF grant AGS-0960497. The author gratefully acknowledges colleagues, Nick Bond, Paulo Ceppi, Greg Johnson, Todd Mitchell, Richard Seager, LuAnne Thompson, and Mike Wallace, whose generous advice and comments greatly improved this contribution. The comments of two anonymous reviewers of an earlier version of this work were extremely helpful.

The Editor thanks Andrew Hoell and an anonymous reviewer for their assistance in evaluating this paper.

References

Alexander, M. A., I. Blade, M. Newman, J. R. Lanzante, N. C. Lau, and J. D. Scott (2002), The atmospheric bridge: The influence of ENSO teleconnections on air-sea interaction over the global oceans, *J. Clim.*, *15*(16), 2205–2231.

Barnes, E. A. (2013), Revisiting the evidence linking Arctic amplification to extreme weather in midlatitudes, *Geophys. Res. Lett.*, *40*, 4734–4739, doi:10.1002/grl.50880.

Barsugli, J. J., and D. S. Battisti (1998), The basic effects of atmosphere-ocean thermal coupling on midlatitude variability, *J. Atmos. Sci.*, *55*(4), 477–493.

Blunden, J., and D. S. Arndt (2014), State of the climate in 2013, *Bull. Am. Meteorol. Soc.*, *95*(7), S1–S257.

Bond, N. A., J. E. Overland, M. Spillane, and P. Stabeno (2003), Recent shifts in the state of the North Pacific, *Geophys. Res. Lett.*, *30*(23), 2183, doi:10.1029/2003GL018597.

Bretherton, C. S., M. Widmann, V. P. Dymnikov, J. M. Wallace, and I. Blade (1999), The effective number of spatial degrees of freedom of a time-varying field, *J. Clim.*, *12*, 1990–2009.

Cayan, D. R. (1992), Latent and sensible heat flux anomalies over the northern oceans: The connection to monthly atmospheric circulation, *J. Clim.*, *5*, 354–369.

Ceballos, L. I., E. Di Lorenzo, C. D. Hoyos, N. Schneider, and B. Taguchi (2009), North Pacific Gyre Oscillation synchronizes climate fluctuations in the eastern and western boundary systems, *J. Clim.*, *22*(19), 5163–5174, doi:10.1175/2009jcli2848.1.

Chhak, K. C., E. Di Lorenzo, N. Schneider, and P. F. Cummins (2009), Forcing of low-frequency ocean variability in the northeast Pacific, *J. Clim.*, *22*(5), 1255–1276, doi:10.1175/2008jcli2639.1.

Compo, G. P., et al. (2011), The Twentieth Century Reanalysis Project, *Q. J. R. Meteorol. Soc.*, *137*(654), 1–28, doi:10.1002/qj.1776.

Cummins, P. F., and H. J. Freeland (2007), Variability of the North Pacific current and its bifurcation, *Progr. Oceanogr.*, *75*(2), 253–265, doi:10.1016/j.pocean.2007.08.006.

Davis, R. E. (1976), Predictability of sea-surface temperature and sea-level pressure anomalies over the North Pacific Ocean, *J. Phys. Oceanogr.*, *6*(3), 249–266.

Deser, C., and M. L. Blackmon (1995), On the relationship between tropical and North Pacific sea-surface temperature variations, *J. Clim.*, *8*(6), 1677–1680.

Deser, C., A. Phillips, V. Bourdette, and H. Y. Teng (2012), Uncertainty in climate change projections: The role of internal variability, *Clim. Dyn.*, *38*(3–4), 527–546, doi:10.1007/s00382-010-0977-x.
Di Lorenzo, E., et al. (2008), North Pacific Gyre Oscillation links ocean climate and ecosystem change, *Geophys. Res. Lett.*, *35*, L08607, doi:10.1029/2007GL032838.
Ding, Q. H., J. M. Wallace, D. S. Battisti, E. J. Steig, A. J. E. Gallant, H. J. Kim, and L. Geng (2014), Tropical forcing of the recent rapid Arctic warming in northeastern Canada and Greenland, *Nature*, *509*(7499), 209–212, doi:10.1038/nature13260.
Eade, R., D. Smith, A. Scaife, E. Wallace, N. Dunstone, L. Hermanson, and N. Robinson (2014), Do seasonal-to-decadal climate predictions underestimate the predictability of the real world?, *Geophys. Res. Lett.*, *41*, 5620–5628, doi:10.1002/2014GL061146.
Francis, J. A., and S. J. Vavrus (2012), Evidence linking Arctic amplification to extreme weather in mid-latitudes, *Geophys. Res. Lett.*, *39*, L06801, doi:10.1029/2012GL051000.
Frankignoul, C., N. Sennechael, Y. O. Kwon, and M. A. Alexander (2011), Influence of the meridional shifts of the Kuroshio and the Oyashio Extensions on the atmospheric circulation, *J. Clim.*, *24*(3), 762–777.
Horel, J. D., and J. M. Wallace (1981), Planetary-scale atmospheric phenomena associated with the Southern Oscillation, *Mon. Weather Rev.*, *109*, 813–829.
Huber, M., and R. Knutti (2014), Natural variability, radiative forcing and climate response in the recent hiatus reconciled, *Nat. Geosci.*, *7*(9), 651–656, doi:10.1038/ngeo2228.
Kalnay, E., et al. (1996), The NCEP/NCAR 40-Year Reanalysis Project, *Bull. Am. Meteorol. Soc.*, *77*(March), 437–471.
Kim, B.-M., S.-W. Son, S.-K. Min, J.-H. Jeong, S.-J. Kim, X. Zhang, T. Shim, and J.-H. Yoon (2014), Weakening of the stratospheric polar vortex by Arctic sea-ice loss, *Nat. Commun.*, *5*, doi:10.1038/ncomms5646.
Kosaka, Y., and S. P. Xie (2013), Recent global-warming hiatus tied to equatorial Pacific surface cooling, *Nature*, *501*(7467), doi:10.1038/nature12534.
Kushnir, Y., W. A. Robinson, I. Blade, N. M. J. Hall, S. Peng, and R. Sutton (2002), Atmospheric GCM response to extratropical SST anomalies: Synthesis and evaluation, *J. Clim.*, *15*(16), 2233–2256.
Kwon, Y. O., M. A. Alexander, N. A. Bond, C. Frankignoul, H. Nakamura, B. Qiu, and L. Thompson (2010), Role of the Gulf Stream and Kuroshio-Oyashio systems in large-scale atmosphere-ocean interaction: A review, *J. Clim.*, *23*(12), 3249–3281.
Lau, N. C., and M. J. Nath (1994), A modeling study of the relative roles of tropical and extratropical SST anomalies in the variability of the global atmosphere-ocean system, *J. Clim.*, *7*(8), 1184–1207.
Lau, N. C., and M. J. Nath (1996), The role of the "atmospheric bridge" in linking tropical Pacific ENSO events to extratropical SST anomalies, *J. Clim.*, *9*(9), 2036–2057.
Liu, Z. Y., and M. Alexander (2007), Atmospheric bridge, oceanic tunnel, and global climatic teleconnections, *Rev. Geophys.*, *45*, RG2005, doi:10.1029/2005RG000172.
Mantua, N. J., and S. R. Hare (2002), The Pacific Decadal Oscillation, *J. Oceanogr.*, *58*(1), 35–44.
Mantua, N. J., S. R. Hare, Y. Zhang, J. M. Wallace, and R. C. Francis (1997), A Pacific interdecadal climate oscillation with impacts on salmon production, *Bull. Am. Meteorol. Soc.*, *78*(6), 1069–1079.
Miller, A. J., D. R. Cayan, and W. B. White (1998), A westward-intensified decadal change in the North Pacific thermocline and gyre-scale circulation, *J. Clim.*, *11*(12), 3112–3127.
Neelin, J. D., D. S. Battisti, A. C. Hirst, F.-J. Fei, Y. Wakata, T. Yamagata, and S. E. Zebiak (1998), ENSO theory, *J. Geophys. Res.*, *103*(C7), 14,261–14,290, doi:10.1029/97JC03424.
Newlin, M. L., and M. C. Gregg (2014), Global oceans [in "State of the Climate in 2013"], *Bull. Am. Meteorol. Soc.*, *95*(7), S51–S78.
North, G., T. Bell, R. Cahalan, and F. Moeng (1982), Sampling errors in the estimation of empirical orthogonal functions, *Mon. Weather Rev.*, *110*, 699–706.
Palmer, T. N., and D. L. T. Anderson (1994), The prospects for seasonal forecasting—A review paper, *Q. J. R. Meteorol. Soc.*, *120*(518), 755–793.
Qiu, B. (2000), Interannual variability of the Kuroshio Extension system and its impact on the wintertime SST field, *J. Phys. Oceanogr.*, *30*(6), 1486–1502.
Rasmusson, E. M., and J. M. Wallace (1983), Meteorological aspects of the El Niño/Southern Oscillation, *Science*, *222*, 1195–1202.
Rayner, N. A., D. E. Parker, E. B. Horton, C. K. Folland, L. V. Alexander, D. P. Rowell, E. C. Kent, and A. Kaplan (2003), Global analyses of sea surface temperature, sea ice, and night marine air temperature since the late nineteenth century, *J. Geophys. Res.*, *108*(D14), 4407, doi:10.1029/2002JD002670.
Seager, R., and M. Hoerling (2014), Atmosphere and ocean origins of North American droughts, *J. Clim.*, *27*(12), 4581–4606.
Seager, R., Y. Kushnir, N. H. Naik, M. A. Cane, and J. Miller (2001), Wind-driven shifts in the latitude of the Kuroshio-Oyashio Extension and generation of SST anomalies on decadal timescales, *J. Clim.*, *14*(2001), 4249–4265.
Seager, R., M. Hoerling, S. Schubert, H. Wang, B. Lyon, A. Kumar, J. Nakamura, and N. Henderson (2014), Causes and predictability of the 2011–14 California drought, *Rep.*, 40 pp., doi:10.7289/V7258K7771F.
Smirnov, D., M. Newman, and M. A. Alexander (2014), Investigating the role of ocean-atmosphere coupling in the North Pacific Ocean, *J. Clim.*, *27*(2), 592–606.
Smith, T. M., R. W. Reynolds, T. C. Peterson, and J. Lawrimore (2008), Improvements to NOAA's historical merged land-ocean surface temperature analysis (1880–2006), *J. Clim.*, *21*(10), 2283–2296.
Trenberth, K. E., and J. T. Fasullo (2013), An apparent hiatus in global warming?, *Earth's Future*, *1*(1), 19–32.
Vimont, D. J., D. S. Battisti, and A. C. Hirst (2001), Footprinting: A seasonal connection between the tropics and mid-latitudes, *Geophys. Res. Lett.*, *28*(20), 3923–3926, doi:10.1029/2001GL013435.
Vimont, D. J., J. M. Wallace, and D. S. Battisti (2003), The seasonal footprinting mechanism in the Pacific: Implications for ENSO, *J. Clim.*, *16*(16), 2668–2675.
Vivier, F., K. A. Kelly, and L. Thompson (1999), Contributions of wind forcing, waves, and surface heating to sea surface height observations in the Pacific Ocean, *J. Geophys. Res.*, *104*(C9), 20,767–20,788, doi:10.1029/1999JC900096.
Wang, F. Y., Z. Y. Liu, and M. Notaro (2013), Extracting the dominant SST modes impacting North America's observed climate, *J. Clim.*, *26*(15), 5434–5452, doi:10.1175/jcli-d-12-00583.1.
Wang, S. Y., L. Hipps, R. R. Gillies, and J.-H. Yoon (2014), Probable causes of the abnormal ridge accompanying the 2013–2014 California drought: ENSO precursor and anthropogenic warming footprint, *Geophys. Res. Lett.*, *41*, 3220–3226, doi:10.1002/2014GL059748.
Zhang, Y., J. M. Wallace, and D. S. Battisti (1997), ENSO-like interdecadal variability: 1900–93, *J. Clim.*, *10*(5), 1004–1020.